CHAPTER FOUR : RESULTS ANALYSIS AND MODELING

4.0 Introduction

The effective minority carrier recombination lifetime for the effects of metal contamination and thermal oxidation under accumulated UV irradiation will be presented in this chapter. The transient recovery of effective minority carrier recombination lifetime after UV irradiation will also be discussed. Finally, a model is proposed to explain the change of effective minority carrier recombination lifetime under accumulated UV irradiation.

4.1 Metal Contamination Results

The spiking concentrations of metal in the dipping solution and the concentration of metallic contaminant on the wafer surface as measured by the AAS are shown in Table 4.1. Two set of wafers with "high" ($>20 \times 10^{10}$ atoms/cm^2) and "low" ($<20 \times 10^{10}$ atoms/cm^2) contamination levels are produced using two different spiking concentrations. Generally, the contaminant concentration on the wafer surface is doubled when using twice the spiking concentration. These spiking concentrations with "high" and "low" contamination levels on the wafer surface were prepared based on previous report[121].

The electronegativity of metal may be used to explain different metal contaminant concentrations on the Si wafer surface as shown in Table 4.1. These electronegativities decrease from 1.9 for Cu to 1.5 for Al. Si has a electronegativity of

about 1.8. Chemical interaction is more likely to occur when the more the electronegativity of a metal compared to Si. This may be correlated to concentration on the Si wafer surface which increases from Cu to Al. By comparing Cu and Al, 5.0 and 0.5 ppb of their spiking concentrations were needed to obtain the surface contaminant concentrations of 10.0 and 16.4 x 10^{10} atoms/cm^2 respectively.

Contaminant	Electronegativity	Spiking concentration / ppb	Concentration on surface / 10^{10} atoms/cm^2
Copper (Cu)	1.9	5.0	10.0
		10.0	22.2
Nickel (Ni)	1.8	0.5	12.4
		2.0	48.9
Iron (Fe)	1.8	0.5	13.8
		1.0	20.7
Zinc (Zn)	1.6	0.5	16.7
		1.0	30.3
Aluminium (Al)	1.5	0.5	16.4
		1.0	35.0

Table 4.1 : Metal contaminants on the silicon wafer surface introduced by solution with different spiking concentrations.

There are several reports on the differential deposition rates of Al and Fe from solution into the wafer surface[115,133-137]. They concluded that the physical absorption are possible for the contaminants which can precipitate easily. Two hypothesis were proposed by them to explain the deposition of Al on Si surface. Firstly, the chemical affinity of aluminates with the Si-OH on the silicon dioxide is greater than Fe, secondly, the precipitated Al hydroxide is very stable. This is evident

in this work as shown in Table 4.1 comparing Al (35.0 x 10^{10} atoms/cm^2) and Fe (20.7 x 10^{10} atoms/cm^2) for 1.0 ppb spiking concentration.

4.1.1 Effective Minority Carrier Recombination Lifetime under Accumulated UV Irradiation

The value of effective minority carrier recombination lifetime in the Si wafer contaminated with five different metals under accumulated UV irradiation are shown in Figures 4.1 to 4.5. The effective minority carrier recombination lifetime in uncontaminated wafer is presented as a reference. The uncontaminated wafer has gone through the same preparation process but without any contaminant in the spiking solution.

Figures 4.1 and 4.2 show that the effective minority carrier recombination lifetimes for "low" contaminant levels of Al and Ni do not change significantly from that of the uncontaminated wafer. However, at the "high" contamination levels of Al and Ni, they show significant departure. The change in the effective minority carrier recombination lifetimes are also observed for both "low" and "high" contamination levels of Zn and Fe, but in those two cases, their lifetimes for "low" and "high" contamination levels do not differ much. In comparison, the initial rate of rise in the effective minority carrier recombination lifetime is much faster for "high" contamination levels of Al and Ni than those of Zn and Fe. However, the effective minority carrier recombination lifetime for Al/Ni pairs saturates earlier at about 100 min of accumulated UV irradiation, whereas those of Al and Ni, the lifetime increases monotonialy to higher values.

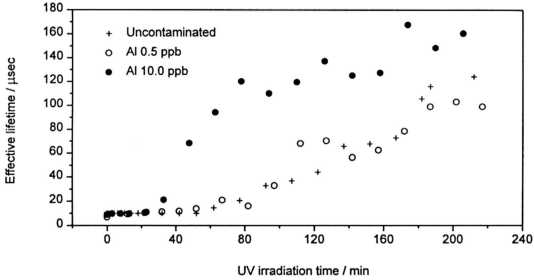

Figure 4.1 : A plot of effective minority carrier recombination lifetime against accumulated UV irradiation time in 0.5 and 10.0 ppb Al-contaminated wafers.

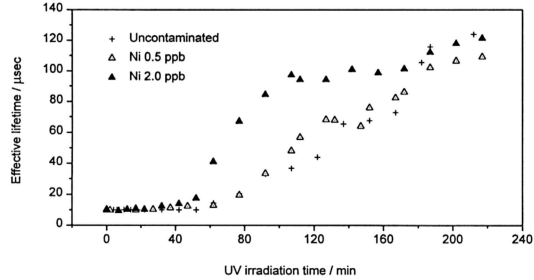

Figure 4.2 : A plot of effective minority carrier recombination lifetime against accumulated UV irradiation time in 0.5 and 2.0 ppb Ni-contaminated wafers.

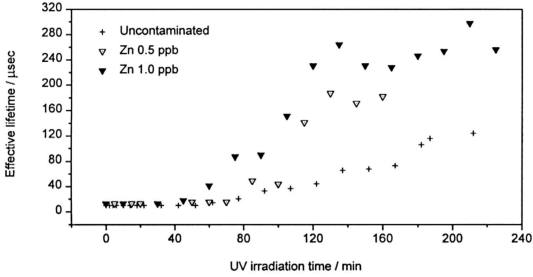

Figure 4.3 : A plot of effective minority carrier recombination lifetime against accumulated UV irradiation time in 0.5 and 1.0 ppb Zn-contaminated wafers.

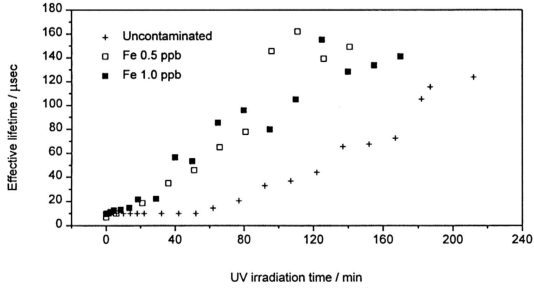

Figure 4.4 : A plot of effective minority carrier recombination lifetime against accumulated UV irradiation time in 0.5 and 1.0 ppb Fe-contaminated wafers.

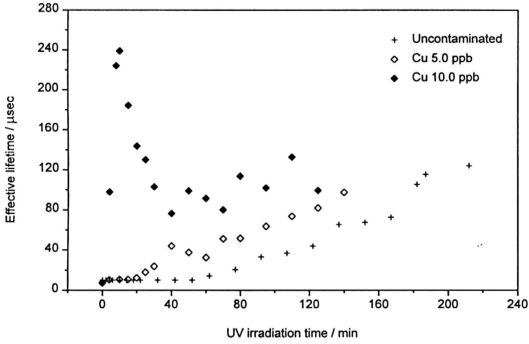

Figure 4.5 : A plot of the effective minority carreir recombination lifetime against accumulated UV irradiation time in 5.0 and 10.0 ppb Cu-contaminated wafers.

In the case of Cu as shown in Figure 4.5, the effective minority carrier recombination lifetime increases steadily for 5.0 ppb but increases drastically to 240 μs and then reduces to 80 μs in the case of 10.0 ppb. This fast changing of effective minority carrier recombination lifetime in 10.0 ppb of Cu contamination could relate to high diffusibility of Cu into the silicon bulk[138]. It may also due to the UV enhanced diffusion of Cu into the bulk of wafer. Cu introduces a recombination center in the bulk which will decrease the bulk recombination lifetime.

The minimum accumulated UV-irradiation duration before the onset of the effective minority carrier recombination lifetime increase is called the "threshold time" as shown in Table 4.2 for different metal contaminants. For an uncontaminated wafer, the threshold time is consistently about 60 min. In general, the threshold times are reduced as the spiking concentration increases. In 10 ppb Cu and 1.0 ppb Fe, the effective minority carrier recombination lifetime increases instantaneously after UV irradiation, hence, no entries were made in Table 4.2 for these two cases.

4.1.2 Transient Recovery of Effective Minority Carrier Recombination Lifetime after UV Irradiation

The effective minority carrier recombination lifetime will increase beyond the threshold time under accumulated UV irradiation. When the UV source is switched off, the effective minority carrier recombination lifetime starts to decrease to its initial value as before UV irradiation. This decrement of effective minority carrier recombination lifetime process is called "transient recovery".

Contaminant	Electronegativity	Spiking concentration / ppb	Threshold time / min
Clean	-	None	60
Cu	1.9	5.0	15
		10.0	0*
Ni	1.8	0.5	50
		2.0	32
Fe	1.8	0.5	9
		1.0	0*
Zn	1.6	0.5	52
		1.0	30
Al	1.5	0.5	60
		1.0	50

* - the effective minority carrier recombination lifetime increase immediately after UV irradiation.

Table 4.2 : The threshold time in the effective minority carrier recombination lifetime of Si wafer with different metal

Several mechanisms for the transient recovery of effective minority carrier recombination lifetime have been suggested, which are listed as follow :

(I) Recombination of electrons on the surface with "fast states" at the interface, this process is dominated by ≡Si-OH bonds which act as intermediate states in the electron recombination processes[28].

(ii) Tunneling of electrons on the surface through a very thin native oxide layer (13Å ~ 20Å) into silicon substrate.

(iii) Thermal detrapping[120] of thermally activated carriers after UV irradiation through defects[118,119] in Si-SiO_2 and native oxide which decreases with surface roughness[116,117].

(vi) Loss of electrons from the wafer surface into the atmosphere.

The transient recovery of the effective lifetime for the contaminated wafer is shown in Figure 4.6 for the uncontaminated wafer. The transient recovery of effective minority carrier recombination lifetime is approximately of an exponential form following equation 4.1 below

$$\tau_{eff}(t) = \tau_{eff}(\infty) + [\ \tau_{eff}(0) - \tau_{eff}(\infty)\ ]\ exp[-kt] \qquad (4.1)$$

where $\tau_{eff}(0)$ and $\tau_{eff}(\infty)$ are the effective lifetimes when UV source is switched off and before UV irradiation respectively; k is the decay rate constant. Hence, this decay rate constant is being used to compare the decay rates of effective minority carrier recombination lifetime of two different accumulated UV irradiation time in the "low" and "high" metal contaminated wafers are shown in Figures 4.7(a) to (e) and 4.7(f) to (i) respectively.

In the Figure 4.7, the value of k for contaminated wafer decreases when the accumulated UV irradiation time increases generally. In 0.5 ppb Al, for example, the values of k are 0.19 and 0.14 s^{-1} for the accumulated UV irradiation time of 80 and 125 minutes respectively. However, the value of k for uncontaminated wafer shows no

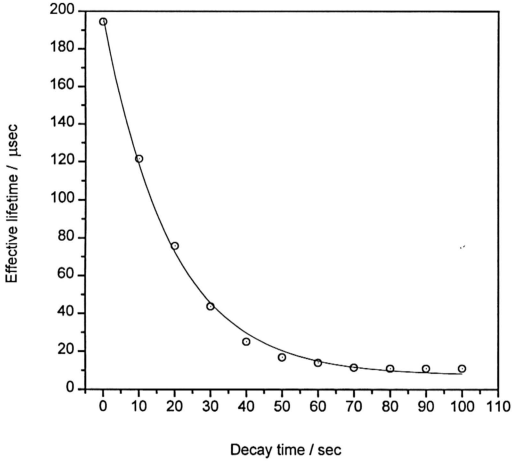

Figure 4.6 :Transient recovery of uncontaminated wafer after UV irradiation.

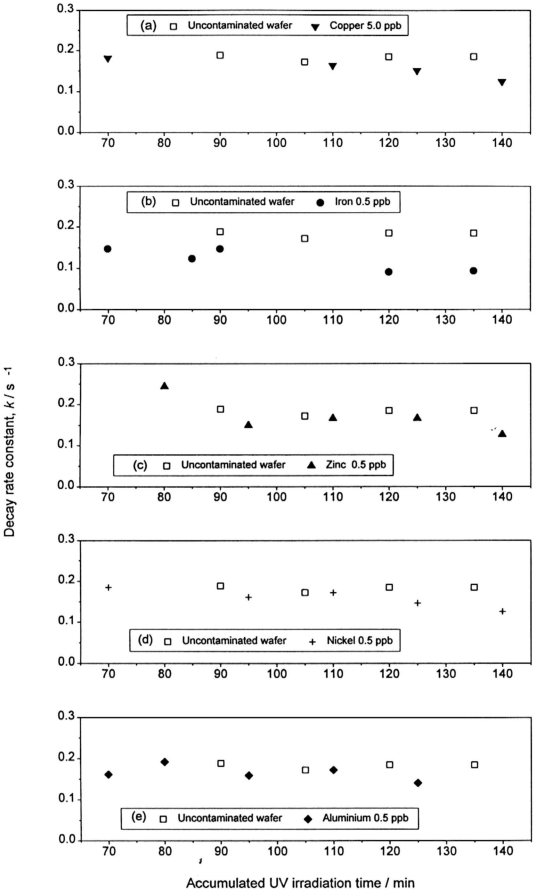

Figure 4.7(a)-(e) : Decay rate constant, *k* for wafer contaminated with 5ppb of (a) Cu and 0.5 ppb of (b) Fe, (c) Zn, (d) Ni and (e) Al.

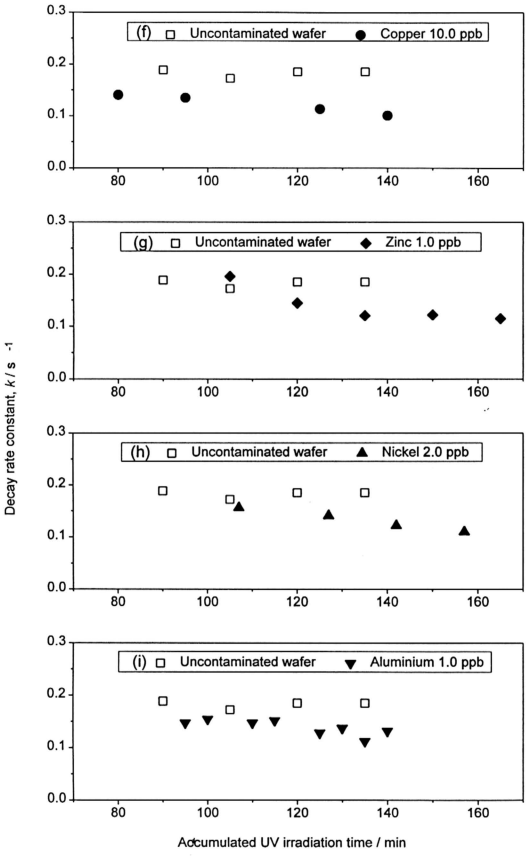

Figure 4.7(f) - (i) : Decay rate constant, k for wafer contaminated with 10 ppb of (f) Cu, 1.0 ppb of (g) Zn, 2.0 ppb of (h) Ni and 1.0 ppb of (i) Al.

significant change as compare to the contaminated wafer from accumulated UV irradiation of 90 to 135 minutes. The decreasing value of *k* indicates that the electrons are more difficult to return to the Si substrate in longer UV irradiation samples. This is agreeable with the mechanisms of recombination of electrons on the surface with "fast states" at the interface whereby bonding can be easily broken by UV. The bond breaking activities may reduce the number of fast states which act as intermediate states in electrons recombination process.

The *k* value of "low" metal contaminated wafer does not change significantly as compare to that of uncontaminated wafer except for 0.5 ppb Fe as shown in Figures 4.7(a) to (e). However, in "high" contaminated wafers, the *k* value departs from that of uncontaminated wafer as shown in Figures 4.7(f) to (i). The complexes formed by metal contaminant on the surface may trap electrons during the recombination process with holes at the surface of Si substrate. They may form negatively charged centers to alter the electron recombination process and the surface potential as reported[122-132].

4.2 Effects of Thermal Silicon Dioxide

The oxidation temperatures and times needed to grow thermal oxide is shown in Table 4.3. Three different oxidation temperatures and six different oxidation times are used to grow the oxide layers on Si wafer surfaces.

After thermal oxidation process, the oxide thickness were measured using an ellipsometer and the results are shown in Table 4.3. The oxide rate of growth is

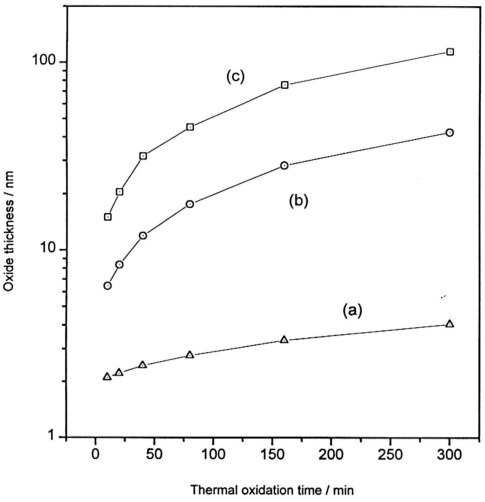

Figure 4.8 : Thickness of the thermal oxide layer grown at the temperature of (a) 700 °C, (b) 900 °C and (c) 1000 °C.

Oxidation Temperature / °C	Time / min	Average thickness / Å
700	10	21.0
	20	22.1
	40	24.3
	80	27.6
	160	33.2
	300	40.4
900	10	64.6
	20	83.7
	40	119.4
	80	175.8
	160	283.6
	300	425.1
1000	10	150.1
	20	207.0
	40	317.2
	80	451.0
	160	756.6
	300	1180.2

Table 4.3 : Thickness of the thermal oxide layer on the Si wafer

depicted in Figure 4.8. The trend of the oxide growth agrees with the linear-parabolic relationship as described by Deal-Grove model[139].

4.2.1 Effective Minority Carrier Recombination Lifetime under Accumulated UV Irradiation

The effective minority carrier recombination lifetime of thermally oxidized wafers under accumulated UV irradiation are shown in Figures 4.9 to 4.11. The effective minority carrier recombination lifetimes for thermal oxide grown at temperature, T_0 = 700 °C and oxidation time, t_0 of 10, 20, 80 and 160 min decrease to around 50 μsec

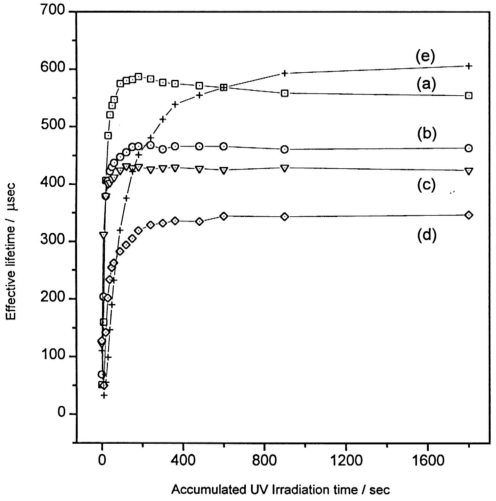

Figure 4.9 : A plot of effective minority carrier recombination lifetime versus accumulated UV irradiation time for samples with oxide layer prepared thermally at 700,°C for (a) 10 min, (b) 20 min, (c) 80 min, (d) 160 min and (e) 300 min.

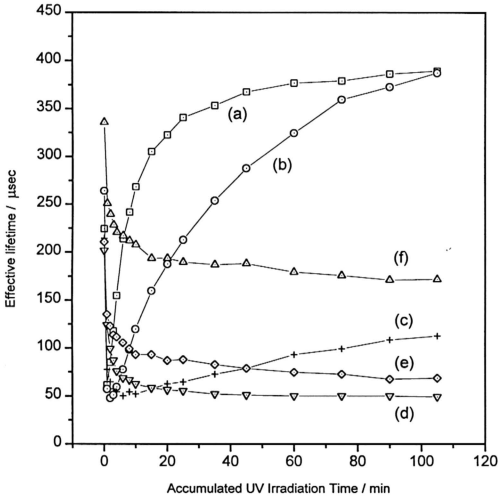

Figure 4.10 : A plot of effective minority carrier recombination lifetime versus accumulated UV irradiation time for samples with oxide layer prepared thermally at 900 °C and time of (a) 10 min, (b) 20 min, (c) 40 min, (d) 80 min, (e) 160 min and (f) 300 min.

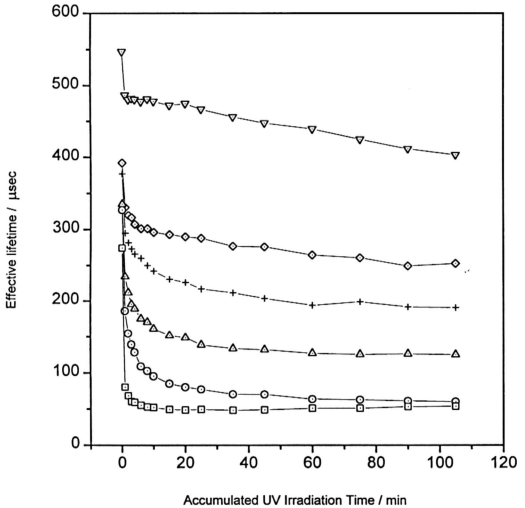

Figure 4.11 : A plot of effective minority carrier recombination lifetime versus accumulated UV irradiation time for samples with oxide layer prepared thermally at 1000 °C for (a) 10 min, (b) 20 min, (c) 40 min, (d) 80 min, (e) 160 min and (f) 300 min.

during the initial stage of UV irradiation and increase again rapidly with further irradiation. However, after 900 sec, the effective minority carrier recombination lifetime reaches saturation as shown in Figure 4.9. The saturation lifetimes decrease with oxidation time from 570 to 344 μsec for t_0 = 10 and 160 min respectively. In the case of t_0 = 10 min, the rapid increment of effective minority carrier recombination lifetime reaches a peak value and gradually decreases slightly toward the saturation value. A different trends is observed for the wafer oxidized at t_0 = 300 min. In this case, the effective minority carrier recombination lifetime decreases to 33 μs but increase again at a slower rate than for the other four cases. The saturation lifetime value for this case however is highest among all other samples.

The change of effective minority carrier recombination lifetime for T_o = 900 °C is shown in Figure 4.10. The effective minority carrier recombination lifetimes decrease rapidly within 5 min of initial stage of UV irradiation. Effective minority carrier recombination lifetime enhancement are shown by those wafers oxidized for t_0 = 10, 20 and 40 min but the rate of enhancement decreases for sample with t_0 = 10 and 40 min of accumulated UV irradiation. No enhancement of lifetime was observed for wafers oxidized for t_0 = 80, 160 and 300 min, on the contrary the lifetimes decrease for these cases. These samples reach an equilibrium effective minority carrier recombination lifetime after approximately 40 min of UV irradiation. The equilibrium move upward for wafer oxidized for t_0 = 80 to 300 min as shown in Figure 4.10.

For wafers oxidized at T_o = 1000°C (Figure 4.11), the effective minority carrier recombination lifetimes decreased with accumulated UV irradiation for all the

oxidized wafers. It is also observed that the equilibrium lifetimes increase with respect to the oxidation time.

The work as discussed in this section was accepted to be published with minor revisions by the Journal of Electrochemical Society in January 1997.

4.2.2 Effective Minority Carrier Recombination Lifetime after UV Irradiation

After irradiation in the UV chamber, the wafer is transported by a robotic arm for measurement of τ_{eff}. The time lag between the end of irradiation and the beginning of measurement is 12 seconds. The transient recovery curves as recorded after the final accumulated UV irradiation cycle for the wafers oxidized at T_0 = 700°C shows a decay constant in the order of days (Figure 4.12). Hence during the 12 seconds period taken to transport the wafer, the effective minority carrier recombination lifetimes for the samples studied do not change significantly and should be close to the value immediately after irradiation.

The transient recovery can be attributed to a discharging process. At 4.9 eV, the UV irradiation is sufficiently energetic to excite the electrons in the Si across the SiO_2 barrier. The surface charging brings about a surface potential change, bends the energy band, alters surface recombination velocity, S_r and hence also the effective minority carrier recombination lifetime. The rate of the transient recovery observed will then be related to how the surface charge is depleted. If the discharge occurs due to electrons returning to the Si substrate through the oxide layer, then, it is reasonable that the transient recovery for thicker oxide would be longer. This appears to be

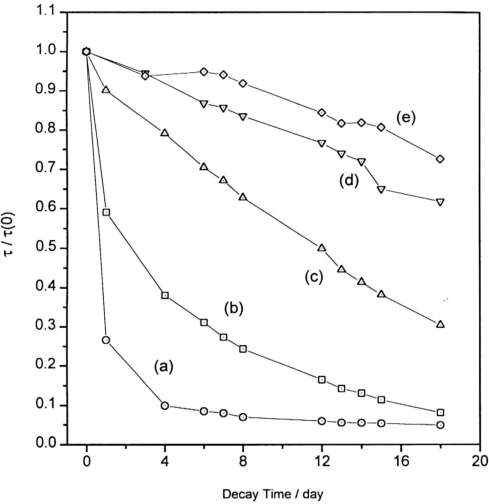

Figure 4.12 : Normalized recovery time versus decay time for samples with oxide layer prepared at 700 °C and time of (a) 10 min, (b) 20 min, (c) 40 min, (d) 80 min and (e) 160 min.

consistent with what is observed for the case of wafers oxidized at T_0 = 700 °C (Figure 4.12), that is, wafers which are oxidized for a longer period of time and hence with thicker oxides exhibit longer transient recovery time.

Charge retention mechanisms may also affect the transient recovery process, for example trapping of electrons by electronic traps within the oxide and also attraction of the surface electrons by adsorbed oxygen. However, it is not possible to directly determine from this experiment the significance of these other mechanism in the transient recovery process.

For the wafers oxidized at T_0 = 900 and 1000°C, no transient recovery was observed. Their effective minority carrier recombination lifetime after accumulated UV irradiation appears to be relatively stable. Over a 20 day period when the effective minority carrier recombination lifetime of these wafers were being monitored, no significant lifetime changes were observed. In this case, the surface charging and discharging effect may be small and hence over time, no appreciable change in the effective minority carrier recombination lifetime was observed.

4.3 Proposed Mechanism of UV-Irradiated Effect on Silicon Wafer Surface

In this section we describe a simple two-species model which employs a combination of surface defect interconversion and band-bending as shown in Figure 4.13 and 4.14 respectively which may be used to describe the behaviors of the effective minority carrier recombination lifetime under accumulated UV irradiation. The positive oxide charges are located inside the oxide layer[37,39] of the sample. Owing to these

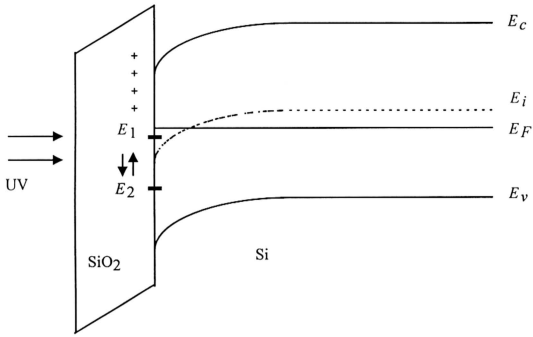

Figure 4.13 : Silicon wafer surface defect interconversion

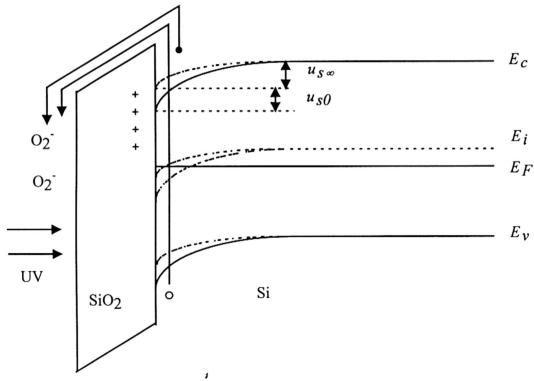

Figure 4.14 : Energy band banding

positive oxide charges, the conduction and valence bands bend downward. The holes are repelled into the bulk while electrons are accumulated at the surface of the sample, forming a depletion layer below the oxide layer. During the UV irradiation, the change of these two effects can affect the surface recombination velocity, S_r (eqn (2.1)), and hence, the effective minority carrier recombination lifetime, τ_{eff} (eqn (2.11)).

In this model, the surface defect interconversion involves only two localized energy states of E_1 and E_2 which may be introduced by the defects, dangling bonds or complexes in the energy gap of Si-SiO_2 interface. These two surface localized energy states are represented by the species 1 and 2 with the concentration of N_1 and N_2 respectively as shown in Figure 4.13. Both species 1 and 2 are located below the Fermi level, E_F . However, species 1 is located nearer to the Fermi level and hence more effective recombination center in the recombination processes. Before UV irradiation, no species 1 will be converted into species 2, the total number of surface localized energy state, n_t is therefore equal to N_1.

During UV irradiation, species 1 may be converted to species 2 or vice versa. The inter-conversion between species 1 and species 2 are shown below

$$\text{Species 1} \underset{k_2}{\overset{k_1}{\rightleftharpoons}} \text{Species 2} \qquad (4.2)$$

where k_1 and k_2 are the rate constants. From equation (4.2), the rate of change of species 2 is given by

$$\frac{dN_2}{dt} = k_1 N_1 - k_2 N_2 \tag{4.3}$$

and the total number of surface localized energy state is

$$n_t = N_1 + N_2 \tag{4.4}$$

By substituting equation (4.3) into (4.4), one can obtain

$$N_1(t) = n_t \{ 1 - c [1 - e^{-(k_1 + k_2) t}] \} \tag{4.5}$$

$$N_2(t) = c\, n_t \{ 1 - e^{-(k_1 + k_2) t} \}$$

where $$c = \frac{k_1}{k_1 + k_2}$$

The concentration of species 1 and 2 is a function of UV irradiation time. For the longer UV irradiation time, more of the species 1 will be converted to species 2. However, the rate and the saturation number of species 1 converted to species 2 are determined by the rate constants of k_1 and k_2.

Other than the defect inter-conversion during the accumulated UV irradiation, electrons in the valence band are also excited by the 4.9 eV photons (from fixed-energy UV source) into the conduction band of SiO_2[80]. This energy is sufficient to move an electron from the Si substrate to the SiO_2 layer resulting in a charged surface[29-32,37]. The oxygen molecules adsorbed on the oxide surface may attract some of these electrons. The negative charge which bends the energy band upward

altering the level of the surface localized energy states relative to the Fermi level. Assuming that the surface charging is a capacitor charging effect, the bending rate may be estimated to be an exponential form, hence, the change of the normalized surface potential, u_S as a function of the UV irradiation time is given as

$$u_S(t) = \frac{qV_s}{kT} = u_{S\infty} + u_{S0}\, e^{-k_3 t} \tag{4.6}$$

where, as shown in Figure 4.14, u_{s0} and $u_{s\infty}$ are the normalized surface potentials; k_3 is the bending rate constant; k is the Boltzmann constant and T is the absolute temperature.

By substituting $N_t(t)$ and $u_S(t)$ (eqs (4.5) and (4.6)) into $S_r(t)$ (eqn. (2.1)), the surface recombination velocity as a function of UV irradiation time can be expressed as

$$S_r(t) = \frac{Kn_t\,(p_b + n_b)\{1 - c[1 - e^{-(k_1+k_2)\,t}]\}}{2n_i\{\cosh[\frac{E_F - E_i}{kT}] + \cosh[u_{s\infty} + u_{s0}e^{-k_3 t}]\}} \tag{4.7}$$

where the capture probabilities of the electron and hole are given by

$$K_n = K_p = K$$

Hence, the change of effective lifetime under accumulated UV irradiation can be determined by solving the equation (2.11) where the surface recombination velocity is given by equation (4.7).

4.3.1 Modeling of the Effective Minority Carrier Recombination Lifetime of Metal Contaminated Wafers

The metallic contaminants in Si wafer can change the total number of surface localized energy states, n_t . It may form complexes with the Si and O atoms on the surface of the wafer[81-88]. UV irradiation on the wafer surface then convert the species 1 into species 2 as a function of the irradiation time. In a Si wafer with a natural oxide layer, almost all the species 1 are converted into species 2 by the 4.9 eV UV photons.

The effective minority carrier recombination lifetimes, τ_{eff} of contaminated wafers under accumulated UV irradiation using the proposed two species model with different total number of surface localized energy states, n_t are plotted in Figures 4.15 to 4.19 using equation (2.13) of special case II in Section 2.3. The values for the parameter k_1, k_2 and n_t are shown in Table 4.4. In Figures 4.15 to 4.19, the effective lifetime does not change significantly before the threshold time. Beyond the threshold time, it starts to increase to reach its saturation value.

The profiles of the lifetime curve in Figures 4.15 to 4.19 derived from the simple model compare well with the wafers contaminated with Al, Zn and Ni but not for Fe and Cu. The threshold time and the lifetime enhancement rate for Al, Zn and Ni are

contaminant	Spiking concentration / ppb	k_1 / min^{-1}	$k_2 \times 10^{-5}$ / min^{-1}	$n_1 \times 10^{15}$ / cm^{-2}
Al	0.5	0.045	11	12
	1.0	0.055	11	11
Zn	0.5	0.050	6	10
	1.0	0.075	11	9
Ni	0.5	0.050	11	14
	2.0	0.080	11	20
Fe	0.5	0.200	3	20
	1.0	0.200	3	170
Cu	5.0	0.350	3	900
	10.0	1.750	3	1000

Assumption : τ_b = 500 μsec L = 550 x 10^{-4} cm

k_3 = 2.0 min^{-1} D_n = 35 cm^2s^{-1}

Table 4.4 : The values of k_1, k_2 and n_1 of the metal contaminated silicon wafer in the modelling of effective minority carrier recombination lifetime under accumulated UV irradiation.

consistent with the model. The fast saturation of effective lifetime derived from the model compare to Fe and Cu 5.0 ppb shows that the interconversion of species may be more complicated involving more than two species. This model is also unable to stimulate the change of effective minority carrier recombination lifetime for Cu 10.0 ppb. This may due to the change of bulk recombination lifetime which is assumed to be constant in this model after Cu is diffused into the bulk.

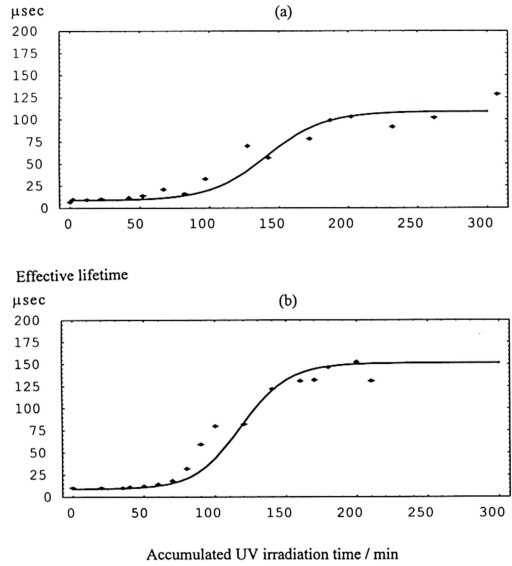

Figure 4.15 : The effective minority carrier recombination lifetime deduced from the model (solid line) and experimental results (scattered points) under accumulated UV irradiation for the samples contaminated with (a) 0.5 ppb and (b) 1.0 ppb of Al.

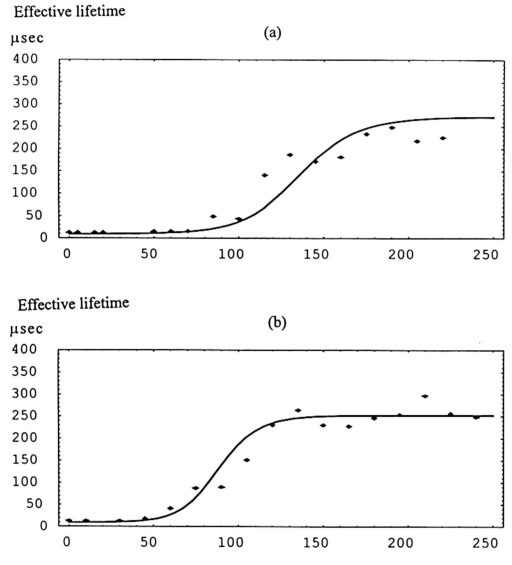

Figure 4.16 : The effective minority carrier recombination lifetime deduced from the model (solid line) and experimental results (scattered points) under accumulated UV irradiation for the samples contaminated with (a) 0.5 ppb and (b) 1.0 ppb of Zn.

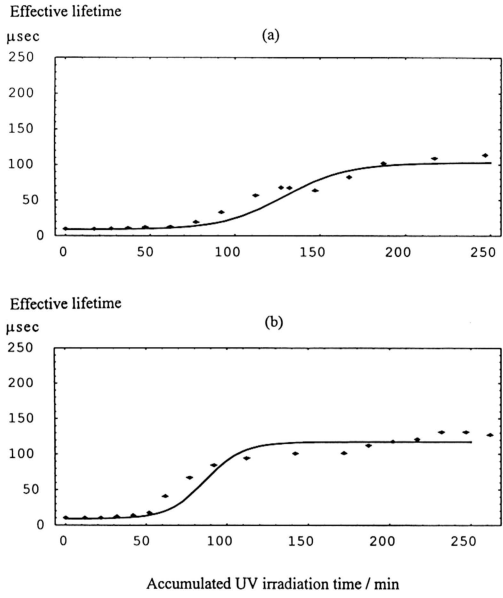

Figure 4.17 : The effective minority carrier recombination lifetime deduced from the model (solid line) and experimental results (scattered points) under accumulated UV irradiation for the samples contaminated with (a) 0.5 ppb and (b) 2.0 ppb of Ni.

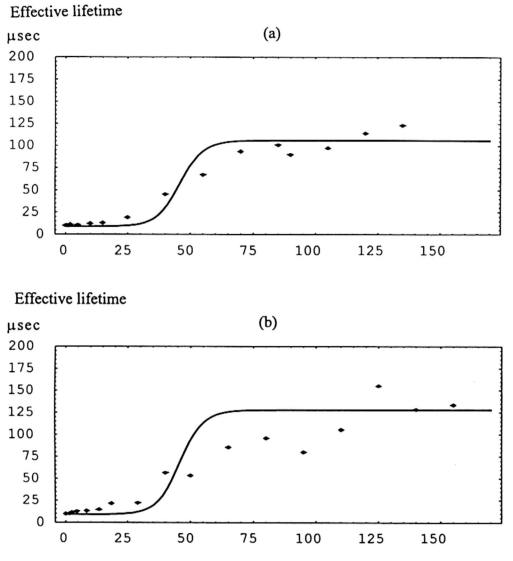

Figure 4.18 : The effective minority carrier recombination lifetime deduced from the model (solid line) and experimental results (scattered points) under accumulated UV irradiation for the samples contaminated with (a) 0.5 ppb and (b) 1.0 ppb Fe.

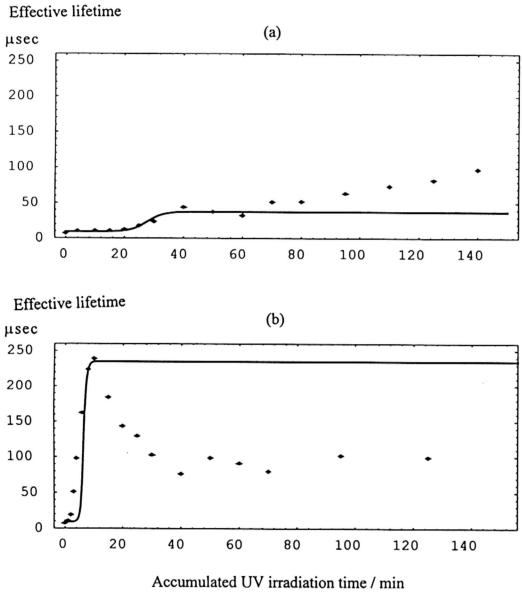

Figure 4.19 : The effective minority carrier recombination lifetime deduced from the model (solid line) and experimental results (scattered points) under accumulated UV irradiation for the samples contaminated with (a) 5.0 ppb and (b) 10.0 ppb Cu.

For the demonstration of how the effective minority carrier recombination lifetime changes under the accumulated UV irradiation in Al, Zn and Ni, the two species model may be adequate to show this general trend for the experimental data obtained in this work. However, this model needs to be improved in the cases of Fe and Cu contaminated wafers..

4.3.2 Modeling of the Effective Minority Carrier Recombination Lifetime of Thermally Oxidized Wafers

In the thermally oxidized wafers, the total number of localized surface energy state, n_t decreases after thermal passivation of the surface. The surface localized energy state at the Si-SiO_2 interface is reduced by the thermal oxide growth in the furnace during the thermal oxidation process. Other than a decrease in the number of traps after surface thermal passivation, it is strongly believed that a smaller number of species 1 will be converted into species 2 at higher oxidation temperature as compared to lower oxidation temperature during UV irradiation. This could be related to the adsorption of UV photons in amorphous oxide layer or interconversion ability in different oxide thicknesses at the interface. Hence, the values of rate constant, k_1 and the total number of localized energy states, n_t will be chosen so that k_1 and n_t reduce from low to high oxidation temperature and duration of oxidation.

The change in the effective minority carrier recombination lifetime of the oxidized wafers under accumulated UV irradiation are plotted in Figures 4.20, 4.21 and 4.22 and are compared to the proposed model for the contaminated wafers in order to

explain the effects of oxidation temperatures at T_0 = 700, 900 and 1000 °C and different oxidation durations respectively. In these three cases, only three parameters, that are, rate constants k_1, k_2 and total number of localized energy state, n_t are varied resulting in the change of effective minority carrier recombination lifetime. The values of these parameters are shown in Table 4.5. In this table, the decrement of rate constant, k_1 and total number of localized energy states, n_t from short to long oxidation time are consistent with the observations and assumptions discussed above.

The profile of the effective minority carrier recombination lifetime curves under accumulated UV irradiation derived from the model and the experimental data (Figures 4.9, 4.10 and 4.11) are shown in Figures 4.20, 4.21 and 4.22 respectively. The drastic decrement during the initial stage of UV irradiation (Figures 4.20(f) and 4.21(a) to (c)) is related to the rate constant of surface potential, k_3, whereas the saturation and the rate of change of effective minority carrier recombination lifetime are governed by the total number of localized energy states, n_t and rate constants k_1 and k_2 as shown in Table 4.5.

The enhancement of the effective minority carrier recombination lifetime from the experimental data (Figure 4.9) towards the saturation values are slower compared to the model prediction and the faster effective minority carrier recombination lifetime decrement rate in the cases of T_0 = 900 and 1000 °C as shown in Figures 4.21 and 4.22 respectively. These differences between experimental results and model predictions may be due to the interconversion of species which is more complicated and involving more than two species may be present in actual situation. However, the

Temperature / °C	Time / min	k_1 / min^{-1}	k_2 / min^{-1}	n_t x 10^8 / cm^{-2}
700	10	6.55	0.015	100.00
	20	6.53	0.050	50.00
	40	6.53	0.023	60.00
	80	5.53	0.060	40.00
	160	3.60	0.072	30.00
	300	1.97	0.010	3.00
900	10	0.28	0.14	3.00
	20	0.13	0.14	2.00
	40	0.024	0.14	2.60
	80	0.0008	0.14	2.10
	160	0.0008	0.14	1.35
	300	0.0008	0.14	0.45
1000	10	0.0008	0.14	2.50
	20	0.0008	0.14	1.70
	40	0.0008	0.14	0.70
	80	0.0008	0.14	0.39
	160	0.0008	0.14	0.24
	300	0.0008	0.14	0.09

Assumption : $\tau_b = 500$ µsec

$D_n = 35\ cm^2s^{-1}$

$L = 550 \times 10^{-4}$ cm

$k_3 = 2.0\ min^{-1}$

$u_{so} = 2.2$

$u_{s\infty} = 2.2$

Table 4.5 : The values of k_1, k_2 and n_t of the oxidised silicon wafers in the modelling of the effective minority carrier recombination lifetime under accumulated UV irradiation.

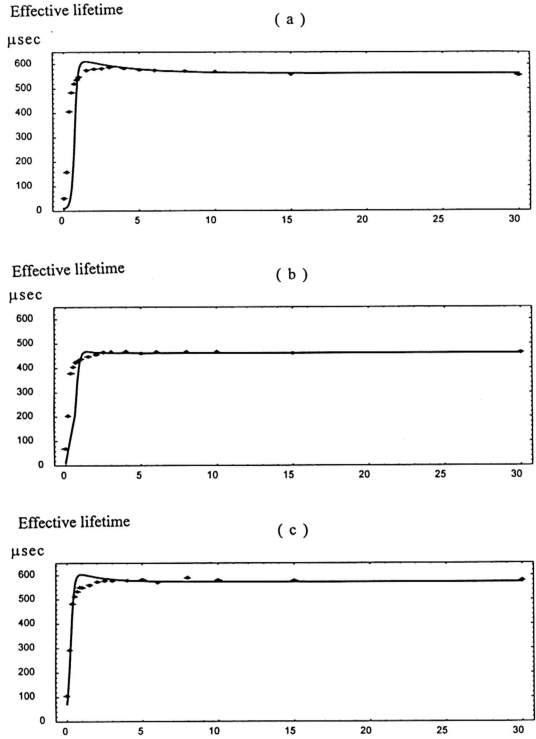

Figure 4.20(a)~(c) : The effective minority carrier recombination lifetime deduced from the model (solid line) and experimental results (scatter points) under accumulated UV irradiation for the samples with oxide layer prepared at 700 °C and time of (a) 10 min, (b) 20 min and (c) 40 min.

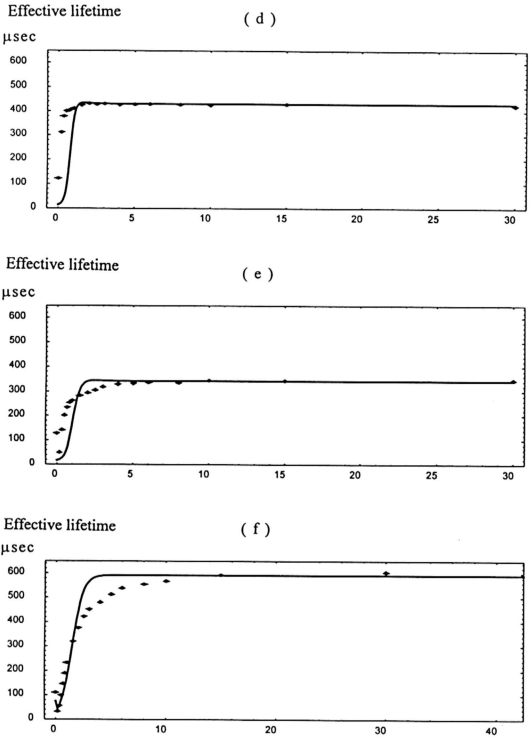

Figure 4.20(d)~(f) : The effective minority carrier recombination deduced from the model (solid line) and experimental results (scatter points) under accumulated UV irradiation for the samples wiht oxide layer prepared at 700 °C and time of (d) 80 min, (e) 160 min and (f) 300 min.

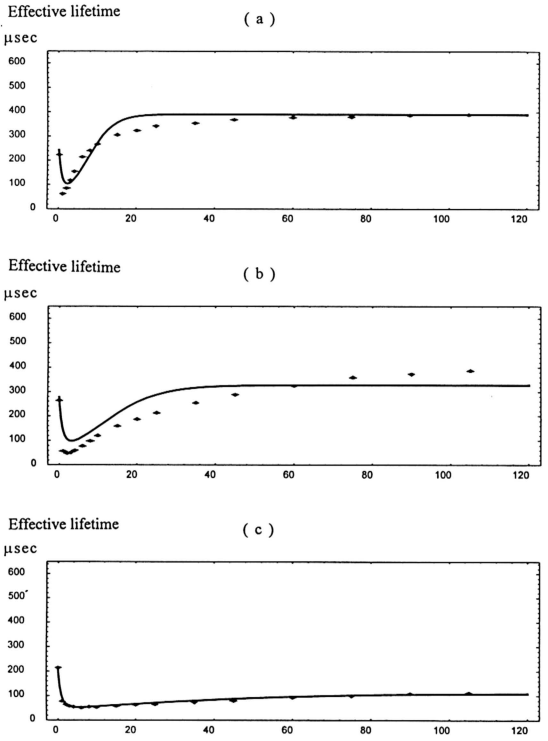

Figure 4.21(a)~(c) : The, effective minority carrier recombination deduced from the model (solid line) and experimental results (scatter points) under accumulated UV irradiation for the samples wiht oxide layer prepared at 900 °C and time of (d) 10 min, (b) 20 min and (c) 40 min.

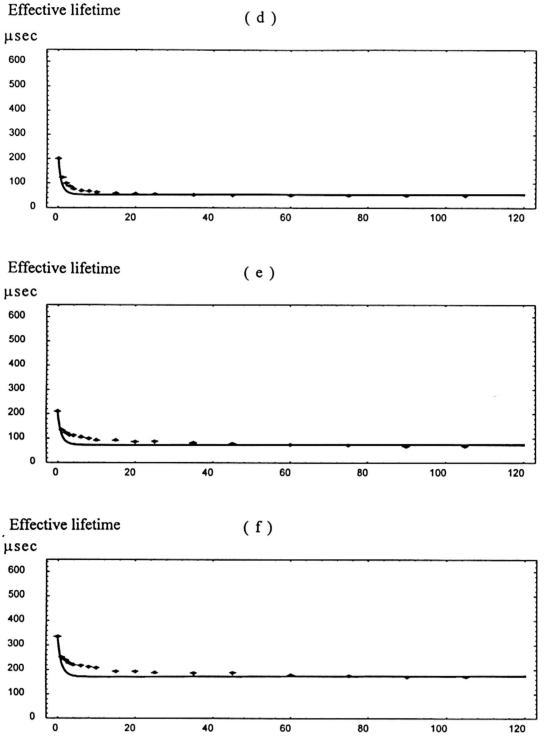

Figure 4.21(d)~(f) : The effective minority carrier recombination deduced from the model (solid line) and experimental results (scatter points) under accumulated UV irradiation for the samples with oxide layer prepared at 900 °C and time of (d) 80 min, (e) 160 min and (f) 300 min.

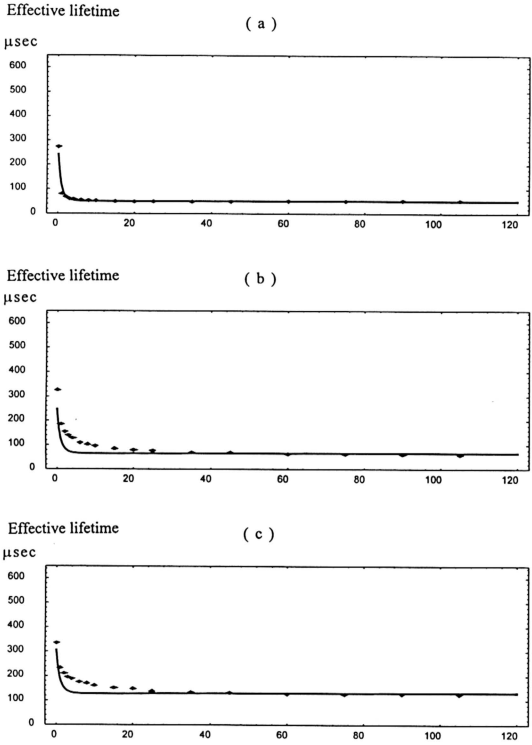

Figure 4.22(a)~(c) : The effective minority carrier recombination deduced from the model (solid line) and experimental results (scatter points) under accumulated UV irradiation for the samples with oxide layer prepared at 1000 °C and time of (d) 10 min, (e) 40 min and (f) 80 min.

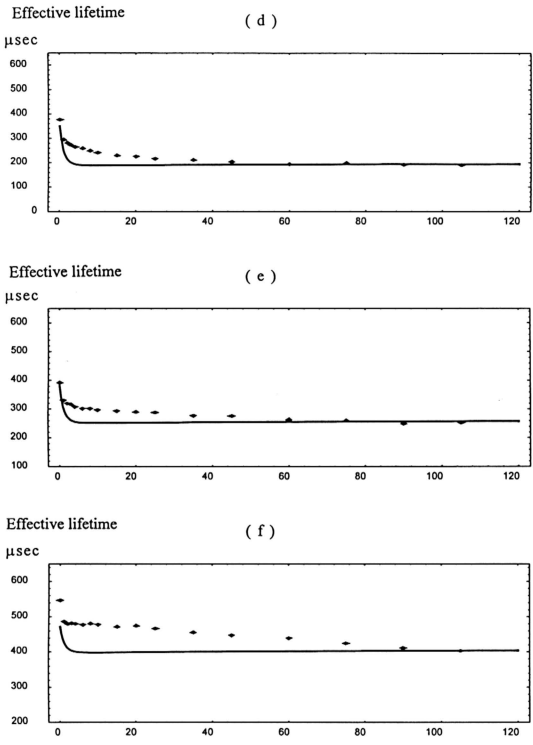

Figure 4.21(d)~(f) : The effective minority carrier recombination deduced from the model (solid line) and experimental results (scatter points) under accumulated UV irradiation for the samples wiht oxide layer prepared at 1000 °C and time of (d) 80 min, (e) 160 min and (f) 300 min.

two-species model may be adequate to show a general trend in the experimental results obtained.

To better understand the interconversion of two species, the rate constants of k_1 and k_2 are used to determine the concentration of species 1 and species 2 (eqn. (2.18)) for long UV irradiation time ($t \rightarrow \infty$). In the case of T_0 = 700 °C and t_0 = 10 min, 99 % of species 1 is converted into species 2, which is below the Fermi level with a fast conversion rate compare to 23 % at T_0 = 1000 °C with same oxidation time. Therefore, for a higher oxidation temperature, there is less probability of species 1 converted into species 2, as a result, the effective minority carrier recombination lifetime for higher temperatures may decrease, as shown in Figure 4.11 for T_0 = 1000 °C.